Time dependence of evanescent quantum waves

J. G. Muga[1,2] and M. Büttiker[1]
[1]*Département de Physique Théorique, Université de Genève, CH-1211, Genève 4, Switzerland*
[2]*Departamento de Química-Física, Universidad del País Vasco, Apartado 644, Bilbao, Spain*
(Received 12 January 2000; published 19 July 2000)

The time dependence of quantum evanescent waves generated by a point source with an infinite or a limited frequency band is analyzed. The evanescent wave is characterized by a forerunner (transient) related to the precise way the source is switched on. It is followed by an asymptotic, monochromatic wave which at long times reveals the oscillation frequency of the source. For a source with a sharp onset the forerunner is exponentially larger than the monochromatic solution and a transition from the transient regime to the asymptotic regime occurs only at asymptotically large times. In this case, the traversal time for tunneling already plays a role only in the transient regime. To enhance the monochromatic solution compared to the forerunner we investigate (a) frequency-band-limited sources and (b) the short-time Fourier analysis (the spectrogram) corresponding to a detector which is frequency band limited. Neither of these two methods leads to a precise determination of the traversal time. However, if they are limited to determine the traversal time only with a precision of the traversal time itself both methods are successful: In this case the transient behavior of the evanescent waves is at a time of the order of the traversal time followed by a monochromatic wave which reveals the frequency of the source.

PACS number(s): 42.50.Ct, 03.65.−w

I. INTRODUCTION

In order to summarize essential aspects of the time dependence of wave phenomena a number of characteristic velocities or times have been defined. The *phase velocity*, ω/k, is the velocity of constant phase points in the stationary wave (assume $k>0$ for the time being)

$$e^{ikx-i\omega t}. \tag{1}$$

The boundary conditions, the superposition principle, and the *dispersion relation* $\omega=\omega(k)$ between the frequency ω and the wave number k determine the time evolution of the waves in a given medium. When a group of waves is formed by superposition of stationary waves around a particular ω, it propagates with the *group velocity* $d\omega/dk$. In *dispersive media* (where ω depends on k), the group velocity can be smaller (normal dispersion) or greater (anomalous dispersion) than the phase velocity. It was soon understood that these velocities could be both greater than c for the propagation of light, and Sommerfeld and Brillouin [1], studying the fields that result from an input step function modulated signal in a single Lorentz resonance medium, introduced other useful velocities, such as the velocity of the very first wavefront (equal to c), or the *signal velocity* for the propagation of the main front of the wave. Both the very first front and the signal velocity describe thus the causal response of the system and are therefore of particular interest.

The above description is, however, problematic for *evanescent waves*, characterized by imaginary wave numbers instead of the real wave numbers of propagating waves. Their time dependence has been investigated by theoreticians and experimentalists in recent years because of its peculiar behavior. A striking phenomenon is that, when crossing an evanescent region, certain initial wave features, such as the peak of the incident amplitude, appear at the far side at anomalously large speeds, but clearly a comparison of peaks of transmitted and incident wave packets does not describe a causal process. Many publications and a recent workshop have been devoted to discuss the implications [2].

The role played by the imaginary part of the group velocity $d\omega/dk$ and the possible definition of a signal velocity in the evanescent case have been much discussed but not yet completely clarified. Assume that a source is placed at $x=0$ and emits with frequency ω_0 from $t=0$ on. If ω_0 is above the *cutoff frequency* of the medium (the one that makes $k=0$) a somewhat distorted but recognizable front propagates with the velocity corresponding to ω_0. Within the framework of the Schrödinger equation, and using a set of dimensionless quantities where the cutoff frequency is 1 (see below), the dispersion relation takes the form [3]

$$\omega=1+k^2, \tag{2}$$

and the signal propagation velocity for the main front is equal to the group velocity, $v_p=(d\omega/dk)_{\omega_0}=2(\omega_0-1)^{1/2}$. In other words, at some distance x form the source, the amplitude behaves, in first approximation, as

$$\psi(x,t)\approx e^{-i\omega_0 t}e^{+ik_0 x}\Theta(t-xv_p), \tag{3}$$

where $k_0=(\omega_0-1)^{1/2}$ is the wave number related to ω_0 by the dispersion relation, and Θ is the Heaviside (step) function. In the evanescent case, $\omega_0<1$, a preliminary analysis by Stevens [4], following the contour deformation techniques used by Brillouin and Sommerfeld, suggested that a main front, moving now with velocity $v_m=2(1-\omega_0)^{1/2}=\mathrm{Im}(d\omega/dk)_{\omega_0}$ and attenuated exponentially by $\exp(\kappa_0 x)$ [where $\kappa_0=(1-\omega_0)^{1/2}$], could be also identified,

$$\psi(x,t)\approx e^{-i\omega_0 t}e^{-\kappa_0 x}\Theta(t-xv_m). \tag{4}$$

The result seemed to be supported by a different approximate analysis of Moretti based on the exact solution [5], and by the fact that the time of arrival of the evanescent front, τ

$=x/v_m$, had been found independently by Büttiker and Landauer [6,7] as a characteristic *traversal time* for tunneling using rather different criteria: semiclassical arguments, the rotation of the electron spin in a weak magnetic field, and the transition from adiabatic to sudden regimes in an oscillating potential barrier.

In the treatment of Stevens, as well as in the original work by Sommerfeld and Brillouin, the contour for the integral defining the field evolution was deformed along the steepest descent path from the saddle point; and the main front (4) was associated with a residue due to the crossing of a pole at $i\kappa_0$ by the steepest descent path. But later, more accurate studies of the punctual source problem or other boundary conditions showed that the contribution from the saddle point (due to frequency components above or at the frequency cutoff created by the sharp onset of the source emission), and possibly from other critical points (e.g., resonance poles when a square barrier is located in front of the source [8]) were generally dominant at τ, so that no sign of the ω_0 front (4) can in fact be seen in the total wave density at that time [8–12]. Similarly, corrections to the original work by Sommerfeld and Brillouin have been also worked out for electromagnetic pulse propagation [13]. In spite of these clarifying works, several important aspects have remained obscure or not investigated, such as the actual time scale for the attainment of the stationary regime, the characterization of the transients, and the role (if any) played by τ in the time dependence of the quantum wave.

Recently, one of the authors in collaboration with Thomas [14], reconsidered the problem of Sommerfeld and Brillouin, and provided a detailed discussion of the forerunners and the signal sent out by a source which has a sharp onset in time. These authors also pointed out that the forerunner, generated by switching on the source, is associated with a time-dependent wide-band spectrum whereas the signal, the ω_0 front, carries the oscillation frequency of the source into the evanescent medium. The signal is called a ''monochromatic front.'' In contrast to previous work, which tried to find a front simply by analyzing the amplitude of the waves, these authors emphasized the frequency content of the forerunner and the signal. In the evanescent case, the amplitude of the monochromatic front is exponentially small compared to the forerunner, and in agreement with the works mentioned above, it cannot be detected using a simple criterion based on the magnitude of the wave. Two approaches were proposed to enhance the monochromatic fronts compared to the forerunners. First, the dominance of the forerunners might arise due to the fact that high frequencies are transmitted in the propagating energy range. This can be avoided if the source is frequency limited such that all frequencies of the source are within the evanescent case. (Technically this means that a frequency window is chosen to avoid the effect of the saddle-point contribution.) A second option is not to limit the source but to frequency limit the detection. We can choose a detector that is tuned to the frequency of the source and that responds when the monochromatic front arrives.

The aim of this work is to characterize the time dependence of Schrödinger evanescent waves generated by a point source. We identify several wave features, in particular the arrival of the first main peak and the transition from a forerunner dominated behavior to an asymptotic behavior dominated by the monochromatic front. We also investigate in some detail the proposals made in Ref. [14] to enhance the monochromatic front and consider both frequency-limited sources and a frequency-time analysis of the wave at a fixed position. This leads to the investigation of the spectrogram of the wave generated by the source.

For a source with a sharp onset, we find that the traversal time τ plays a basic and unexpected role in the transient regime. For strongly attenuating conditions (in the WKB limit) the traversal time governs the appearance of the first main peak of the forerunner. In contrast, the transition from the forerunner to an asymptotic regime which is dominated by the monochromatic signal of the source is given by an exponentially long time. If the source is frequency band limited such that it switches on gradually but is still fast compared to the traversal time, the situation remains much the same as for the sharp source, except that now the transition from the transient regime to the stationary regime occurs much faster, but still on an exponentially long time scale. The situation changes if we permit the source to be switched on over a time scale comparable to or larger than the traversal time for tunneling. Clearly, in this case a precise definition of the traversal time is not possible. But for such a source the transition from the transient regime to the asymptotic regime is now determined by the traversal time. Much the same picture emerges if we limit the detector instead of the source. As long as the frequency window of the detector is made sharp enough to determine the traversal time with accuracy, the detector response is dominated by the uppermost frequencies. In contrast, if the frequency window of the detector is made so narrow that the possible uncertainty in the determination of the traversal time is of the order of the traversal time itself, the detector sees a crossover from the transient regime to the monochromatic asymptotic regime at a time determined by the traversal time.

Possibly, the fact that we cannot determine the traversal time with an accuracy better than the traversal time itself tells us something fundamental about the tunneling time problem and is not a property of the two particular methods investigated here.

Dimensionless quantities and notation

The (dimensional) time-dependent Schrödinger equation for a particle of mass m moving in a constant potential $V(X)=V$ is given by

$$i\hbar\frac{\partial\Psi}{\partial T}=-\frac{\hbar^2}{2m}\frac{\partial^2\Psi}{\partial X^2}+V\Psi. \tag{5}$$

The number of variables and parameters may be reduced by introducing dimensionless quantities for position, time, and wave amplitude,

$$x=\frac{X(2mV)^{1/2}}{\hbar}, \tag{6}$$

$$t=\frac{TV}{\hbar}, \tag{7}$$

$$\psi(x,t)=\frac{\hbar^{1/2}}{(2mV)^{1/4}}\Psi(X,T). \tag{8}$$

This allows us to write the corresponding dimensionless Schrödinger equation,

$$i\frac{\partial\psi}{\partial t}=-\frac{\partial^2\psi}{\partial x^2}+\psi. \tag{9}$$

Other useful dimensionless variables related to the dimensional energy E (or frequency $W=E/\hbar$), and wave number, $K=[2m(W-V/\hbar)/\hbar]^{1/2}$, are, respectively,

$$\omega=E/V, \tag{10}$$

$$k=(\omega-1)^{1/2}=\frac{K\hbar}{(2mV)^{1/2}}. \tag{11}$$

The reader may check that the dimensional dispersion relation

$$W=\frac{V}{\hbar}+\frac{K^2\hbar}{2m} \tag{12}$$

takes for dimensionless quantities the simple form given in Eq. (2).

II. SOURCE WITH A SHARP ONSET (INFINITE FREQUENCY BAND)

In this section we shall investigate the time-dependent wave function for $x\geqslant 0$ and $t>0$ corresponding to the ''boundary condition''

$$\psi(x=0,t)=e^{-i\omega_0 t}\Theta(t), \tag{13}$$

which may also be given by the corresponding Fourier transform

$$\hat{\psi}(x=0,\omega)=\frac{1}{(2\pi)^{1/2}}\frac{i}{\omega-\omega_0+i0}. \tag{14}$$

The superposition

$$\psi(x,t)=\frac{i}{2\pi}\int_{-\infty}^{\infty}d\omega\,\frac{e^{ikx-i\omega t}}{\omega-\omega_0+i0} \tag{15}$$

satisfies the Schrödinger equation as well as the boundary condition (13). Along the integration path, k is positive for $\omega>0$, and purely imaginary (with positive imaginary part) for $\omega<0$. This corresponds to waves that vanish at $x=\infty$. In Ref. [14] the integration was carried out in the complex frequency plane since this permitted a close comparison between the calculation for the Schrödinger equation and for relativistic field equations. If only the Schrödinger equation is of interest the complex k plane is most advantageous. In fact this permits us to express the integral in terms of known functions. In the complex k plane we have

$$\psi(x,t)=-\frac{1}{2i\pi}\int_{\Gamma_+}dk\,2k\frac{e^{ikx-i(k^2+1)t}}{k^2+\kappa_0^2} \tag{16}$$

$$=-\frac{e^{-it}}{2\pi i}\int_{\Gamma_+}dk\left[\frac{1}{k+i\kappa_0}+\frac{1}{k-i\kappa_0}\right]e^{ikx-ik^2t}, \tag{17}$$

where the contour Γ_+ goes from $-\infty$ to ∞ passing above the pole at $i\kappa_0$. The two terms in Eq. (17) lead to integrals with the form discussed in Appendix A. The contour can be deformed along the steepest descent path from the saddle at $k_s=x/2t$, the straight line

$$k_I=-k_R+x/2t \tag{18}$$

(k_R and k_I are the real and imaginary parts of k), plus a small circle around the pole at $i\kappa_0$ after it has been crossed by the steepest descent path, for fixed x, at the critical time

$$\tau=\frac{x}{2\kappa_0}. \tag{19}$$

This procedure allows us to recognize two w functions [15,16] (see Appendixes A and B), one for each integral,

$$\psi(x,t)=\frac{1}{2}e^{-it+ik_s^2t}[w(-u_0')+w(-u_0'')]. \tag{20}$$

Here,

$$u_0'=\frac{1+i}{2^{1/2}}t^{1/2}\kappa_0\left(-i-\frac{\tau}{t}\right),$$

$$u_0''=\frac{1+i}{2^{1/2}}t^{1/2}\kappa_0\left(i-\frac{\tau}{t}\right). \tag{21}$$

It is clear from the exact result [Eqs. (20) and (21)], that τ is an important parameter that appears naturally in the w-function arguments, and determines with κ_0 the global properties of the solution. Its detailed role will be discussed in the following sections.

Equation (20) is in agreement with a previous expression by Moretti [7], derived using different contour deformations and notation. Our analysis of this exact result will be, however, quite different and more detailed.

Approximations

Often an exact expression is not very informative by itself, and the approximations make its essential content manifest in certain limits. The simplest approximation for $\psi(x,t)$ for times before τ is to retain the dominant contribution of

the saddle by setting $k=k_s$ in the denominators of Eq. (17) and integrating along the steepest descent path. It is useful to write this in different ways,

$$\psi_s(x,t)=\frac{e^{-it+ik_s^2t}}{2i\pi^{1/2}}\left(\frac{1}{u_0'}+\frac{1}{u_0''}\right)=\frac{e^{-it+ik_s^2t}\tau(2t/\pi)^{1/2}}{(i-1)\kappa_0(\tau^2+t^2)}$$
$$=\frac{i}{2\pi}\sqrt{\frac{-4\pi i}{\Omega_s t}}\frac{\Omega_s}{\Omega_s-\Omega_0}e^{-i(1-\Omega_s)t}, \qquad (22)$$

where

$$\Omega_s\equiv k_s^2=\frac{x^2}{4t^2}, \quad \Omega_0=-\kappa_0^2. \qquad (23)$$

(These are particular values of the frequency variable $\Omega=\omega-1$, defined with respect to the frequency level of the potential.) The average local instantaneous frequency for this saddle contribution [17] is equal to the frequency of the saddle point,

$$\omega_s\equiv 1+\Omega_s. \qquad (24)$$

(Note the different sign of Ω_s in the exponent of Eq. (22). Ω_s depends on t^{-2} and a time derivative has to be taken to obtain Eq. (24), see [17].)

After the crossing of the pole $i\kappa_0$ by the steepest descent path at $t=\tau$ the residue

$$\psi_0(x,t)=e^{-i\omega_0 t}e^{-\kappa_0 x}\Theta(t-\tau) \qquad (25)$$

has to be added to Eq. (22),

$$\psi(x,t)\approx\psi_s(x,t)+\psi_0(x,t). \qquad (26)$$

The solution given by Eq. (25) describes a monochromatic front that carries the signal into the evanescent medium. The conditions of validity of this approximation can be determined by examining the asymptotic series of the $w(z)$ functions in Eq. (20) for large $|z|$, see Appendix B. In fact, Eq. (26) is obtained from the dominant terms of these expansions. The modulus of the two *w*-function arguments in Eq. (21) is given by

$$M(t)\equiv|-u_0'|=|-u_0''|=\frac{\kappa_0}{t^{1/2}}(t^2+\tau^2)^{1/2}. \qquad (27)$$

This quantity may be large in different circumstances. It goes to ∞ when κ_0, t, or x go to ∞, and also when $t\to 0$. $M(t)$ is minimum at the crossing time $t=\tau$, where it takes the value $M(t=\tau)=(x\kappa_0)^{1/2}$. For $x\kappa<1$ the pole lies within the range of the saddle Gaussian and cannot be treated separately.

Assuming that M is large the phase of z determines the appropriate asymptotic expression of $w(z)$. For $\mathrm{Im}(z)>0$, $w(z)\sim i/(\pi^{1/2}z)$, whereas for $\mathrm{Im}(z)<0$, $w(z)\sim i/(\pi^{1/2}z)+e^{-z^2}$, see Eqs. (B5) and (B6). $\arg(-u_0')$ goes from $\pi/4$ to $3\pi/4$ when t goes from $t=0$ to ∞, and $\arg(-u_0'')$ goes from $\pi/4$, at $t=0$, clockwise to $-\pi/4$ when $t\to\infty$, and crosses the real axis at $t=\tau$. Thus the application of the previous

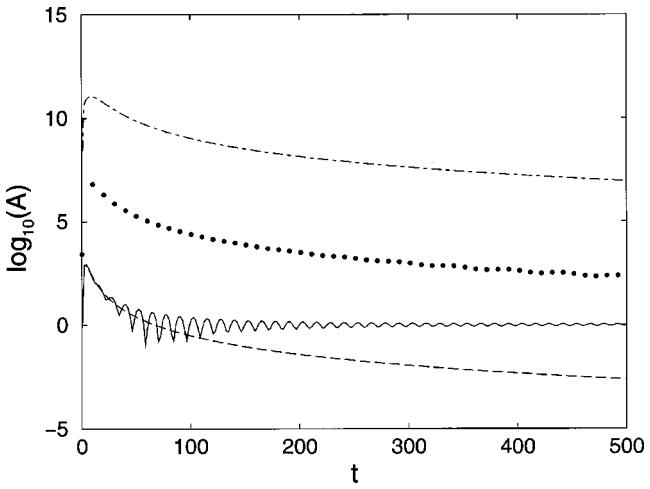

FIG. 1. $\log_{10}$ of the amplified density $A=|\psi(x,t)|^2\exp(2\kappa_0 x)$ versus time for a signal emitted by a source located at $x=0$ with frequency $\omega_0=0.5$, and observed at $x=7,14,21$ (solid, dotted, and dotted-dashed lines). Noticeable for $x=7$ is the contribution of the saddle-point solution ψ_s (dashed line) in comparison with the exact solution ψ. At $x=14,21$ the exact wave function ψ and the saddle-point solution ψ_s are indistinguishable on the scale of the figure. All units are dimensionless.

asymptotic formulas lead exactly to Eq. (26). As discussed in Appendix B one should not be misled by the apparent front in Eq. (26). It is possible to obtain a smooth approximate expression around $t=\tau$ by adding a correction to ψ_s that takes into account the region near the pole [14]. This corrected expression, however, is asymptotically equivalent to Eq. (26) because at τ, and within the conditions that make the saddle approximation valid, the contribution of the pole is negligible. To see this more precisely let us examine the ratio between the modulus of the two contributions,

$$R(t)\equiv\frac{|\psi_0|}{|\psi_s|}=\frac{2\pi^{1/2}}{x}e^{-\kappa_0 x}t^{3/2}(x^2/4t^2+\kappa_0^2). \qquad (28)$$

Its value at τ is an exponentially small quantity,

$$R(t=\tau)=e^{-\kappa_0 x}(2\pi\kappa_0 x)^{1/2}. \qquad (29)$$

Note also that R has a minimum at $\tau/3^{1/2}<\tau$ and tends to ∞ as $t\to\infty$. As a function of x, the minimum of R decreases up to $x\kappa_0=1/2$, and then grows again monotonously.

In summary, for the source with a sharp onset described here, the monochromatic front is not visible when the approximation (26) remains valid around $t=\tau$. However, two very important observable features of the wave can be extracted easily from Eq. (26). The first one is the arrival of the *transient front*, characterized by its maximum density at $t_f\equiv\tau/3^{1/2}$. This time is of the order of τ, but the wave front that arrives does not oscillate with the pole frequency ω_0, but with the saddle-point frequency ω_s. Figure 1 shows this transient front for three positions. In this and similar figures the densities are exponentially amplified by $e^{2\kappa_0 x}$ to make possible the comparison among different values of x with the same scale. Thus, all amplified densities $A\equiv|\psi|^2e^{2\kappa_0 x}$ tend

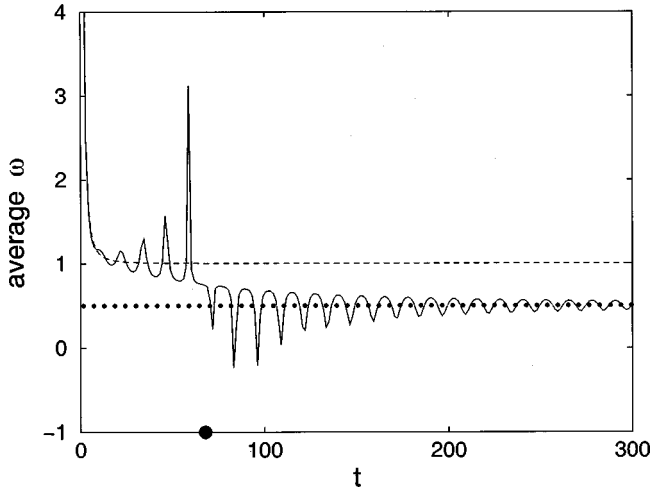

FIG. 2. Evolution of the average instantaneous frequency $\bar{\omega}$, saddle-point frequency ω_s, and signal frequency ω_0 versus time (solid, dashed, and dotted lines) for $x=7$ and $\omega_0=0.5$. The circle marks the time t_{tr} at which the pole contribution and saddle-point contribution are equal in magnitude.

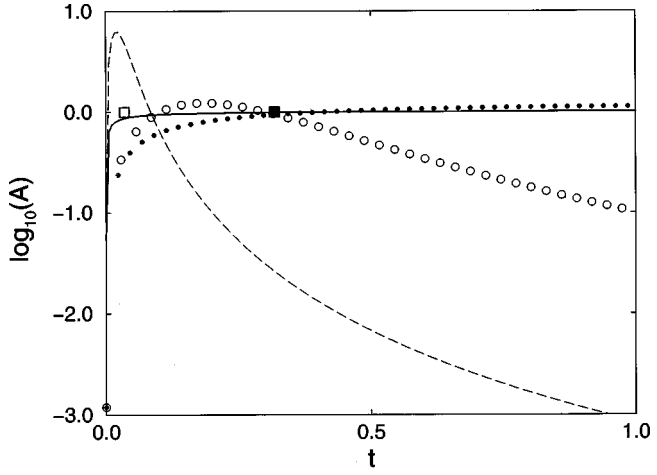

FIG. 3. $\log_{10}$ of the amplified density $A=|\psi(x,t)|^2\exp(2\kappa_0 x)$ versus time for $x=0.05$ and $x=0.45$ (solid and dotted lines, respectively). The approximations provided by the saddle-point solution ψ_s are also shown (dashed line and empty circles). $\omega_0=0.5$. The empty and filled squares mark the values of the traversal time τ for $x=0.05$ and $x=0.45$, respectively.

to one in the asymptotic large-t regime, and the corresponding logarithm to zero. Also shown is the approximation due to ψ_s, although it is only distinguishable from the exact result for $x=7$. Note that the amplified density $|\psi_s|^2 e^{2\kappa_0 x}$ is simply R^{-1}. In Fig. 2 the instantaneous average frequency $\bar{\omega}$ is represented for the smallest x value of Fig. 1, $x=7$. At small t and around the transient front, $\bar{\omega}=\simeq\omega_s$.

The second observable feature that we can extract from Eq. (26) is the time scale for the attainment of the stationary regime, or equivalently, the duration t_{tr} of the transient regime dominated by the saddle before the pole dominates. t_{tr} can be identified formally as the time where the saddle and pole contributions are equal, $R=1$. Because of Eq. (29) we shall assume $\tau \ll t_{tr}$ to obtain the explicit result

$$t_{tr}\approx\left(\frac{x e^{\kappa_0 x}}{2\kappa_0^2\pi^{1/2}}\right)^{2/3}. \tag{30}$$

Using $\kappa_0 x \gg 1$, the velocity for the motion of the space ''point'' where the transition from transient to stationary behavior (or from saddle to pole) takes place is given by

$$v_{tr}\approx\frac{3}{2\kappa_0 t}. \tag{31}$$

Contrary to the motion of the front maximum, this point does not move with constant velocity. The transition may be observed in various ways. In Fig. 1 the decimal logarithms of the exact (amplified) densities and of their components are represented. The crossing point where $R=1$ may be observed for $x=7$ in the change of behavior of the total wave density. The oscillation around t_{tr} is due to the interference between ψ_0 and ψ_s, and has the characteristic period $T_0 \equiv 2\pi/|\Omega_0|$. In Fig. 2 the crossover between the regime dominated by the saddle frequency and the one dominated by ω_0 is also easily noticeable.

Finally, when $x\kappa_0$ is small ($\lesssim 1$), the saddle approximation describes correctly the very short-time initial growth, but fails around τ because the pole is within the width of the Gaussian centered at the saddle point. The pole cancels part of the Gaussian contribution so that the bump predicted by ψ_s at $\tau/3^{1/2}$ is not seen in this regime. Figure 3 shows the time dependence of the density for two small values of x. τ does not correspond to any sharply defined feature, but provides here a valid rough estimate of the attainment of the stationary regime.

III. FREQUENCY-BAND-LIMITED SOURCE

Thomas and one of the authors [14] recently suggested a way to avoid the dominance of the saddle-point solution over the monochromatic front by limiting the frequency band of the source. Specifically, it was proposed to cut off the ω amplitude (14),

$$\hat{\psi}(\omega,x=0)=\frac{1}{(2\pi)^{1/2}}\frac{i}{\omega-\omega_0+i0}[\Theta(\omega-(\omega_0-\Delta\omega)) - \Theta(\omega-(\omega-\Delta\omega))]. \tag{32}$$

This implies that the emission of the source is not sharply defined as in Eq. (14); see Appendix C. Instead,

$$\psi(x=0,t)=e^{-i\omega_0 t}\left[\Theta(t)-\frac{1}{\pi}\mathrm{Im}\,E_1(-i\Delta\omega t)\right], \tag{33}$$

where E_1 is the exponential integral defined in Eq. (C4). The frequency-band width $\Delta\omega$ may be chosen so that the onset of the source is fast with respect to τ and that all the frequencies in the source are in the evanescent region [14],

$$\frac{2\pi}{\tau}\ll\Delta\omega\ll|\Omega_0|. \tag{34}$$

Later we will see that in fact it is necessary to give up the condition that the source switches on fast compared to the traversal time. Now ''negative times'' are also required to describe the signal growth. For an arbitrary x,

$$\psi(x,t)=\frac{i}{2\pi}\int_{\omega_0-\Delta\omega}^{\omega_0+\Delta\omega}d\omega\,\frac{e^{-i(\omega t-kx)}}{\omega-\omega_0+i0}. \tag{35}$$

In this case the integration technique used in the previous section does not provide an analytical solution. We shall manipulate the integral to facilitate the exact numerical evaluation and the discussion of approximations. Using $\Omega=\omega-1$, Eq. (35) becomes

$$\psi(x,t)=\frac{ie^{-it}}{2\pi}\int_{\Omega_0-\Delta\omega}^{\Omega_0+\Delta\omega}d\Omega\,\frac{e^{-i(\Omega t-kx)}}{\Omega-\Omega_0+i0}. \tag{36}$$

The integrand of Eq. (36) has a saddle point at $\Omega_s=(x/2t)^2$. But since Ω_0 is now negative, a frequency interval chosen according to Eq. (34) now excludes this saddle. It is convenient to introduce the variable $y=\Omega/\Omega_s$ so that the valley-hill structure of the exponent remains constant,

$$\psi(x,t)=\frac{ie^{-it}}{2\pi}\int_{y_-}^{y_+}dy\,\frac{e^{i\lambda\,\mathrm{sgn}(t)(2y^{1/2}-y)}}{y-y_0+i0}. \tag{37}$$

Here,

$$y_0=\Omega_0/\Omega_s,\quad y_\pm=y_0\pm\Delta\omega/\Omega_s,\quad \lambda=|\Omega_s t|. \tag{38}$$

In order to perform contour deformations in the complex y plane it is also necessary to specify that the branch cut for $y^{1/2}$ is set along the positive real axis, and that the saddle is at $y=1$ for $t>0$ (just above the cut) but at $y=e^{2i\pi}$ for $t<0$ (just below). The steepest descent and ascent paths from it are given, in the first Riemann sheet of y, by the sections of the parabolas

$$y_I=\mathrm{sgn}(t)\frac{1}{2}(1-y_R^2)\ \ (\text{descent}), \tag{39}$$

$$y_I=-\mathrm{sgn}(t)\frac{1}{2}(1-y_R^2)\ \ (\text{ascent}), \tag{40}$$

starting from the saddle point. Irrespective of the sign of t the original contour in Eq. (37) is entirely within one of the valleys of the saddle, so that there is no need to take this critical point into account in the contour deformation. The most efficient contour deformation consists of following the steepest descent path from the lower integration extreme y_- downwards to infinity and coming up to the upper integration extreme y_+ following its steepest descent path. If $t>0$ this contour encloses the pole at ω_0 and the corresponding residue has to be included. The extreme points become the critical points of the integral, apart from the pole at ω_0 when $t>0$,

$$\psi(x,t)=D_--D_++\psi_0', \tag{41}$$

where $D_\pm$ (generically D_z) are the integrals from $y_\pm$ to ∞ along the corresponding steepest descent paths, $SDP(z)$,

$$D_z=\frac{ie^{-it}}{2\pi}\int_{SDP(z)}dy\,\frac{e^{i\lambda\,\mathrm{sgn}(t)(2y^{1/2}-y)}}{y-y_0}, \tag{42}$$

and

$$\psi_0'(x,t)=e^{-i\omega_0 t}e^{-\kappa_0 x}\Theta(t). \tag{43}$$

Unlike Eq. (25) the residue is now present at all positive times. Using the generic notation $z=y_\pm$ for any of the two extreme points the steepest descent paths from them and their slopes are given by

$$y_I=\frac{1}{2}\mathrm{sgn}(t)[y_R^4-4y_R^3(1+z)+2y_R^2z(4+3z)-4z^2y_R(1+z)+z^4]^{1/2} \tag{44}$$

$$\frac{\partial y_I}{\partial y_R}=\frac{y_R^3-3y_R^2(1+z)+y_Rz(4+3z)-z^2(1+z)}{2y_I}, \tag{45}$$

$$\left.\frac{\partial y_I}{\partial y_R}\right|_z=\mathrm{sgn}(t)(-z)^{1/2}. \tag{46}$$

In the numerical evaluations the value of y along the path may be obtained by solving for each step

$$dy=dy_I(dy_R/dy_I+i), \tag{47}$$

with the initial condition $y=z$.

Approximations

The leading term in λ^{-1} of Eq. (42) is obtained by integrating from z along the ray with the direction of the steepest descent path at z and taking all functions in the integrand, except the exponential, out of the integral, with their values at z [18],

$$D_z\sim D_z^0\equiv\frac{i}{2\pi\lambda(z-y_0)|z^{-1/2}-1|}e^{-it\omega_z-\kappa_z x}e^{i\theta_z}, \tag{48}$$

where $\omega_z=\omega_\pm=\omega_0\pm\Delta\omega$, $\kappa_z=\kappa_\pm=(1-\omega_\pm)^{1/2}$, and θ_z is the angle of the steepest descent path at z,

$$\theta_z=\pi+\arctan[\mathrm{sgn}(t)(-z)^{1/2}] \tag{49}$$

(the branch of the arctan function between $-\pi/2$ and $\pi/2$ is taken). The modulus of these contributions is given by

$$|D_\pm|=\frac{e^{-x\kappa_\pm}}{2\pi\Delta\omega(t^2+t_\pm^2)^{1/2}}, \tag{50}$$

where

$$t_\pm=\frac{x}{2\kappa_\pm} \tag{51}$$

are the critical times when the steepest descent path from the saddle crosses the extreme points of integration $y_\pm$. Regarding the possibility of making the monochromatic front visible, the frequency-band-limited source eliminates the saddle dominated transient effects, but they are substituted by transients associated with a new critical point: the upper extreme of integration. The actual time for transition to the stationary regime is still larger than τ under semiclassical conditions, but much smaller than that for the sharp onset case. A difference with the infinite frequency band case is that the maximum of $|D_\pm|$ is at $t=0$. This is quite remarkable. A particular feature of the wave, its maximum, appears instantly with zero delay at arbitrarily large distances. One should keep in mind, though, that the buildup of the initial signal has required previously an infinite time, from $t=-\infty$ to $t=0$.

The transient regime previous to the dominance of the pole must be also different from the infinite band case since now there is no saddle-point contribution. The transient is here dominated by the integral D_+ because of the exponential dependencies and by the frequency of the upper integration limit y_+. An analysis similar to the one performed in the infinite frequency-band case can be now performed. Let us compare the contributions from the pole and D_+ by dividing their moduli,

$$R' = \frac{|\psi_0'|}{|D_+|} = e^{(-\kappa_0+\kappa_+)x}[2\pi\Delta\omega(t^2+t_+^2)^{1/2}]. \qquad (52)$$

From the condition $R'=1$ we obtain the new critical time

$$t_{tr}' = \left(\frac{e^{2x(\kappa_0-\kappa_+)}}{4\pi^2\Delta\omega^2} - t_+^2\right)^{1/2} \approx \frac{e^{x(\kappa_0-\kappa_+)}}{2\pi\Delta\omega}, \qquad (53)$$

and the critical velocity

$$v_{tr}' \approx \frac{1}{t(\kappa_0-\kappa_+)}. \qquad (54)$$

They have to be compared with the corresponding quantities for the sharp onset case, Eqs. (30) and (31), respectively. The critical time for the transition depends exponentially on x in both cases, but it arrives exponentially earlier for the frequency-band-limited case. In Fig. 4 the logarithm of the amplified density and of the approximation provided by $|D_+^0|^2$ is represented for two values of x. For $x=50$ the transition time t_{tr} is relatively small and can be seen in the time interval shown. (The oscillation period of the interferences around t_{tr} is now $2\pi/\Delta\omega$.) For $x=135$, t_{tr} is much larger and cannot be seen in the scale chosen; note the well-defined peak at $t=0$. The slight disagreement between the exact result and the approximation provided by D_+^0 is because, for very small times, the slope of the steepest descent path from y_+ is very small and the path passes close to the pole. The pole perturbs the integral in this manner for times such that $\lambda^{-1} < \Delta\omega/\Omega_s$, i.e., $t < 2\pi/\Delta\omega$.

From Eq. (52) we see that the dominance of the monochromatic front at τ and fixed x requires that the magnitude of $(-\kappa_0+\kappa_+)x \approx 1$ or smaller. This can be achieved in two

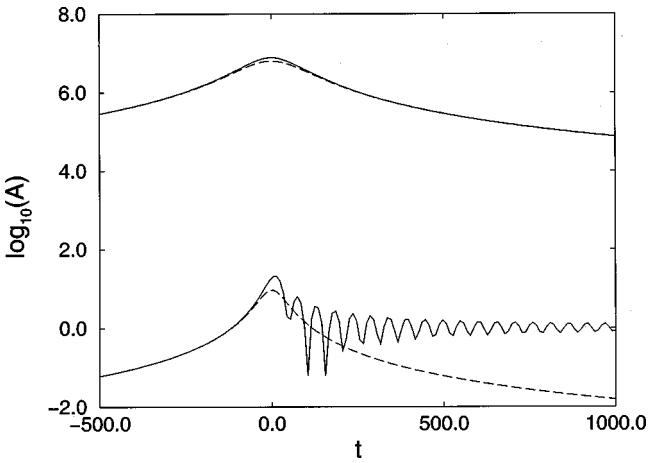

FIG. 4. $\log_{10}$ of the amplified density $A=|\psi(x,t)|^2\exp(2\kappa_0 x)$ for the frequency-band-limited source and of the approximate solution $|D_+^0|^2$ versus time (solid and dashed lines, respectively), for $x=50$ (lower set) and $x=135$ (upper set). $\omega_0=0.5$, $\Delta\omega=0.12$.

ways. (a) We can consider a frequency ω_0 and a frequency interval such that $-\kappa_0$ and κ_+ become small. This means that both $1-\omega_0$ and $\Delta\omega$ should be close to zero, but to avoid propagating waves $\Delta\omega < (1-\omega_0)$. (b) Alternatively, we can allow ω_0 to take any other value below 1, but making the frequency interval $\Delta\omega$ small. In both cases a small frequency window is needed and we can expand with respect to $\Delta\omega$ so that $(-\kappa_0+\kappa_+)x = -\Delta\omega\tau$. Thus we see that the attempt to measure the traversal time accurately has to be abandoned. The lower limit of Eq. (34) is now violated. Figure 5 shows an example where the first inequality in Eq. (34) is not obeyed. The traversal time (rather than t_{tr}, which in this case is an imaginary number) now marks the transition to the asymptotic region even though the buildup time is so large that the arrival of the monochromatic front cannot be defined with a precision better than τ itself. In this respect, Fig. 6 is very illustrative. It shows how the transition of the average frequency characterizing the transient to the frequency of the

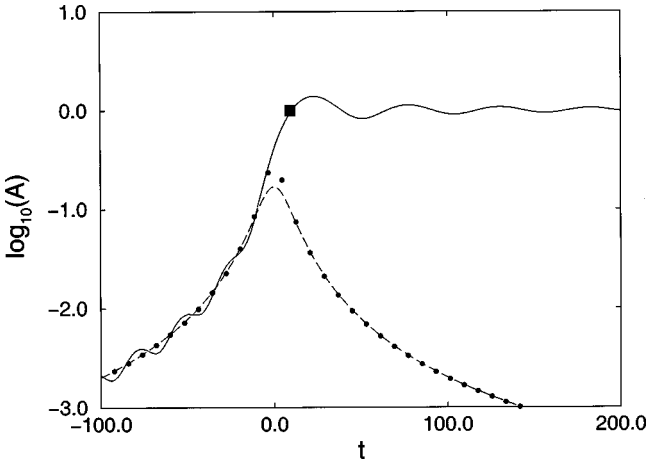

FIG. 5. $\log_{10}$ of the amplified density $A=|\psi(x,t)|^2\exp(2\kappa_0 x)$ of the approximations $|D_+|^2$ and $|D_+^0|^2$ versus time (solid, dashed, and dotted lines, respectively) for $x=13.5$. The square marks the value of τ. $\omega_0=0.5$, $\Delta\omega=0.12$.

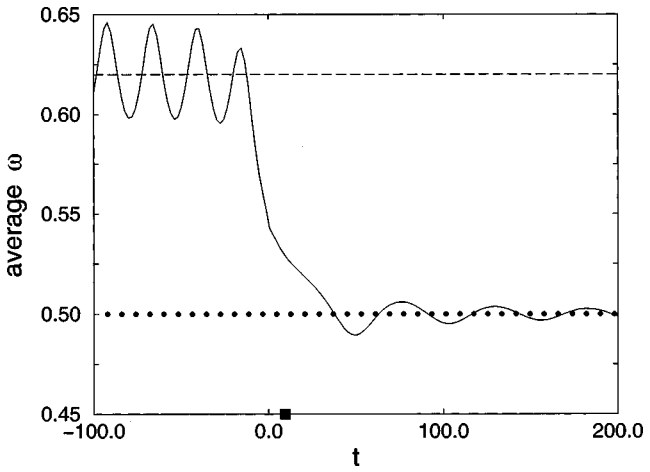

FIG. 6. Frequency evolution $\overline{\omega}$, ω_s, and ω_0 versus time (solid, dashed, and dotted lines) of the frequency-band-limited source for $x=13.5$, $\omega_0=0.5$, and $\Delta\omega=0.12$.

monochromatic solution occurs around the traversal time τ, but the time interval required for the transition is clearly larger than τ.

IV. TIME-FREQUENCY ANALYSIS OF THE WAVE FUNCTION

Instead of limiting the source in frequency we can limit the detection of the field to a range of frequencies of interest [14]. The wave amplitude at fixed position becomes a function of time $\psi(t)$ that can be Fourier analyzed to provide its frequency representation $\hat{\psi}(\omega)$. However, neither of the corresponding densities, $|\psi(t)|^2$ or $|\hat{\psi}(\omega)|^2$, tells when a particular frequency arrives or decays, nor what is the relative importance, at a given time, of different frequency components. This type of information is provided by joint time-frequency representations [19]. There are many possible ways to carry out a time-frequency analysis. A simple one, and surely the most common, is the ''spectrogram,'' based on the short-time Fourier transform (stFt). We are interested in the Fourier spectrum that would be measured at the observation point x if the wave is observed during a time interval of duration T. If a precise determination of the traversal time is attempted, the extent of the time interval T is chosen to be short compared to the traversal time τ. On the other hand, if T is too short then the frequency resolution will be poor. A compromise to obtain a good resolution in time and frequency is for T to be bound above and below [14],

$$\frac{2\kappa_0}{x}=\frac{1}{\tau}\ll\frac{1}{T}\ll\frac{|\Omega_0|}{2\pi}=\frac{\kappa_0^2}{2\pi}. \tag{55}$$

This is equivalently expressed in terms of inequalities for time scales

$$\tau\gg T\gg T_0, \tag{56}$$

where $T_0\equiv 2\pi/|\Omega_0|$ is the oscillation period corresponding to the frequency $|\Omega_0|$. Combining the inequalities one finds $\kappa_0 x\gg 1$; namely, when these conditions are satisfied the saddle contribution to the wave function will be a very good approximation to the total wave up to an ''exponentially long'' time $t_{tr}\gg\tau$, see Sec. II.

The short-time Fourier transform (stFt) of the field $\psi(x,t)$ is given by

$$F(\omega;x,t)=\frac{1}{(2\pi)^{1/2}}\int_{t-T/2}^{t+T/2}dt'\,\exp(i\omega t')\psi(x,t'). \tag{57}$$

Note that the short-time Fourier spectrum depends, in addition to the frequency, parametrically on the observation point x and the time t.

Consider now first the contribution of the monochromatic front to the stFt. We denote this stFt by $F_p(\omega;x,t)$. For $t<\tau-T/2$ we have $F_p(\omega;x,t)=0$. For $t>\tau+T/2$ we find

$$F_p(\omega;x,t)=\frac{2}{(2\pi)^{1/2}}e^{-\kappa_0 x}e^{i(\omega-\omega_0)t}\frac{\sin[(\omega-\omega_0)T/2]}{(\omega-\omega_0)}. \tag{58}$$

This amplitude peaks at the frequency of the source ω_0 and, for $t>\tau+T/2$, it is time independent at this frequency. Away from this frequency the stFt of the monochromatic wave decays algebraically and oscillates sinusoidally. In the time interval $\tau-T/2<t<\tau+T/2$ the stFt tracks the arrival of the monochromatic front,

$$F_p(\omega;x,t)=\frac{ie^{-\kappa_0 x}}{(2\pi)^{1/2}}\frac{1-e^{i(t+T/2)(\omega-\omega_0)}}{\omega-\omega_0}. \tag{59}$$

Consider next the saddle-point contribution. Its frequency in a short-time interval is determined by the expansion of $\Omega_s(t')t'$ away from t. This expansion gives $\Omega_s(t')t'=2\Omega_s(t)t-\Omega_s(t)t'+O((t'-t)^2)$. Taking into account that the prefactors are slowly varying over the time interval of interest here [this is assured by the first inequality in Eq. (55)], we obtain

$$F_s(\omega;x,t)=\frac{i}{\pi}\sqrt{\frac{-2i}{\Omega_s t}}\frac{\Omega_s}{\Omega_s-\Omega_0}\times e^{i(\Omega_s-1+\omega)t}\frac{\sin[(\Omega_s+1-\omega)T/2]}{(\Omega_s+1-\omega)}. \tag{60}$$

The stFt of the saddle-point solution peaks at the frequency $\omega_s\equiv\Omega_s+1$. This frequency is very large at short times (''kinetic regime''), where $\omega_s\sim\Omega_s=x^2/(4t^2)$ is dominated by frequencies above the potential. At long times (''potential regime'') ω_s tends to the potential frequency 1. The transition time between these two regimes of different ω_s can be estimated by solving $\Omega_s(t)=1$. This gives $t=x/2$, which may be larger or smaller than τ. We see that the two Fourier transforms peak at well-separated frequencies. Still the stFt of the pole has an exponentially small amplitude compared to that of the forerunner. Therefore, it is possible that the stFt of the saddle is still large at the frequency ω_0, where the stFt

of the monochromatic front peaks. Thus we have to investigate the stFt of the saddle at the frequency ω_0. From Eq. (60) we obtain

$$F_s(\omega_0;x,t)=\frac{i}{\pi}\sqrt{\frac{-2i}{\Omega_s t}}\frac{\Omega_s}{\Omega_s-\Omega_0}\times e^{i(\Omega_s+\Omega_0)t}\frac{\sin[(\Omega_s-\Omega_0)T/2]}{(\Omega_s-\Omega_0)}. \quad (61)$$

At a time $t=\tau$ the amplitude of the saddle is still of order 1. Thus even at the peak frequency of the front its contribution to the spectrum is of order 1 and much larger than the exponentially small peak of the monochromatic front.

Let us now investigate the properties of the transient in the frequency-time domain, and determine the role played by τ, in particular at the frequency of the signal ω_0. The spectrogram is defined as the square modulus of the stFt, $S(t,\omega;x)=N|F(\omega;x,t)|^2$, where N is a normalization constant. (The notation of the argument of S is appropriate for a time-frequency analysis at fixed x.) For ''normalizable'' cases N is chosen so that $\int\int dt\, d\omega\, S=1$. In our case, this is not possible because the asymptotic stationary regime does not decay, but S provides anyway information on the relative importance of two time-frequency points, so N is chosen to be some convenient value, $N=\pi^2/2$.

For analyzing the transient we may neglect the monochromatic front and concentrate on the saddle-point term. The spectrogram of the saddle-point solution is denoted by $S_s(t,\omega;x)$ and is given by

$$S_s(t,\omega;x)=\alpha(t)\frac{\sin^2[(\Omega_s+1-\omega)T/2]}{(\Omega_s+1-\omega)^2} \quad (62)$$

with an amplitude

$$\alpha(t)=\frac{1}{t}\frac{\Omega_s}{(\Omega_s-\Omega_0)^2}. \quad (63)$$

Note that $\alpha(t)$ is also proportional to the absolute square of the saddle-point solution $|\psi_s(x,t)|^2=(4/\pi)\alpha(t)$. The amplitude α has a maximum as a function of time at the transient front peak, $t_f=3^{-1/2}\tau$, that moves with a speed

$$v_f=\sqrt{3}v_m. \quad (64)$$

Thus v_f determines both the speed of the peak value of the saddle-point solution $|\psi_s(x,t)|^2$ and the speed of the absolute maximum of the spectrogram. The peak value of the spectrogram for a given time is at the frequency $\omega_s=\Omega_s+1$; see an example in Fig. 7. Consider next the spectrogram at the frequency of the source, $\omega=\omega_0$. For fixed x it is bounded by the envelope function

$$\beta(t)=\frac{\Omega_s}{t(\Omega_s-\Omega_0)^4}, \quad (65)$$

and has local maxima close to the times at which the sin function is ± 1. $\beta(t)$ grows as t^5 for short times and decays as t^{-3} for large times. Its maximum arrives, for fixed x, at $\sqrt{5/3}\tau$. Equivalently, this maximum moves with a speed

$$v_{env}=\sqrt{3/5}v_m. \quad (66)$$

This reveals that, in $S(t,\omega_0;x)$, τ is not the time where the stationary regime begins (it is necessary to wait an exponentially long time to attain that regime), but the basic time scale for the arrival of the main part of the transient. The detailed oscillatory pattern of this main part will depend on the value of T/T_0; see Figs. 8 and 9. For $\omega=\omega_0$ the sine function vanishes at times

$$t_n=\frac{\tau}{(nT_0/T-1)}. \quad (67)$$

(In the ω-t plane the spectrogram has a maximum which follows the line $\omega=\Omega_s+1$ and vanishes along the lines $\omega=\Omega_s+1+2\pi n/T$. In between these zero lines the spectrogram exhibits local maxima.) The n for the closest zero to τ is $n\approx 2T/T_0$ whereas the largest t_n [associated with the minimum n so that Eq. (67) has a real solution] corresponds to

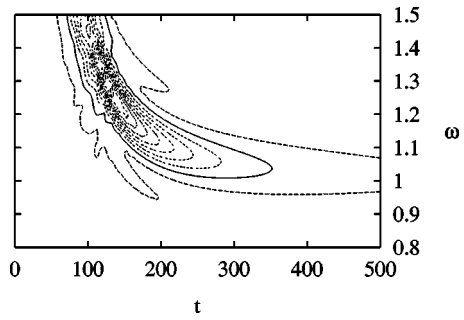

FIG. 7. Contour map of the spectrogram for $\omega_0=0.5$, $T=52.36$, $x=135$. Notice the transition from the kinetic to the potential regime and the side wings around the main peak.

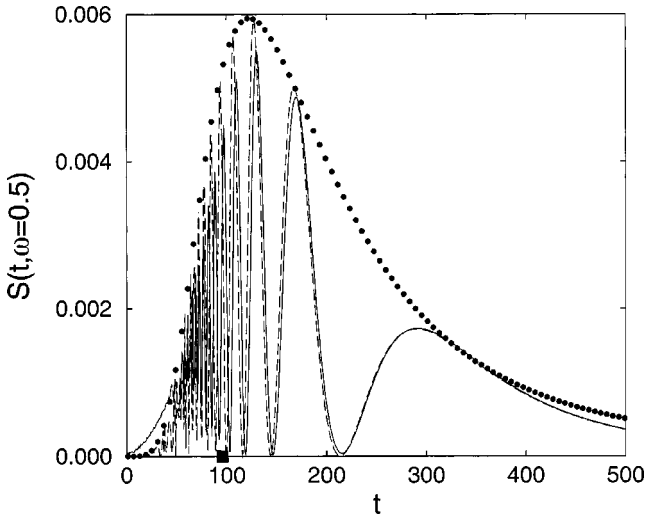

FIG. 8. Spectrogram $S(t,\omega=0,5)$ for $\omega_0=0.5$, $T=52.36$, $x=135$ (solid line). The square marks the value of $\tau=95.4$. (This is the period that corresponds to $\Delta\omega=0.12$ in Fig. 4.) $T_0=12.57$. Also shown, $\beta(t)$ (dotted line) and S_s (dashed line).

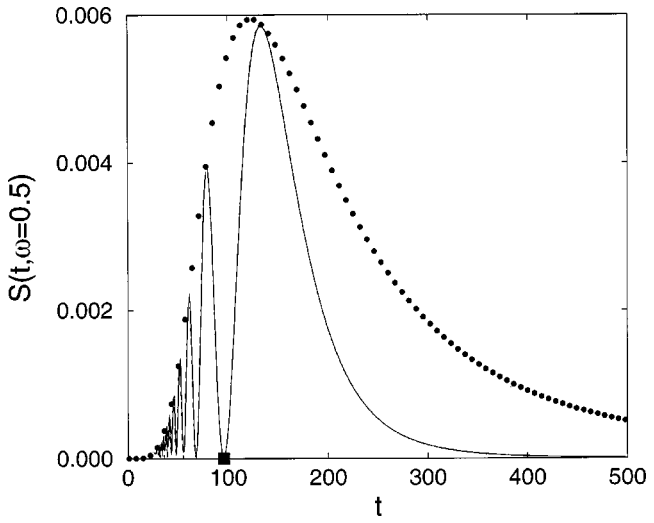

FIG. 9. Spectrogram $S(t,\omega=0,5)$ for $\omega_0=0.5$, $T=12.57$, $x=135$ (solid line). The square marks the value of $\tau=95.4$. $T_0=12.57$. Also shown, $\beta(t)$ (dotted line). S_s is indistinguishable from S.

$n\approx T/T_0$. Hence there are approximately T/T_0 zeros between τ and the last oscillation. For $T/T_0<1$ there is a single major bump close to τ, and for $T/T_0\gg 1$ there are many local maxima that ''sample'' the form of the envelope function (65).

Other time-frequency distributions

The time-frequency characterization of the wave function at a fixed position depends on the quasidistribution chosen. There is nothing wrong with this nonuniqueness as long as the quasidistribution chosen is specified. In choosing the distribution one may consider several factors. Ideally the distribution should be easy to calculate, and should not be too noisy, e.g., with wild oscillations. It may also occur that one of the distributions is naturally adapted to the way the detection experiment is performed.

Let us first discuss a different type of spectrogram. The roles of time and frequency can be inverted so that instead of limiting the Fourier transform of $\psi(t)$ with a ''square window''

$$h(t)=\Theta(t-T/2)\Theta(-t-T/2), \tag{68}$$

a ''short frequency Fourier transform'' (sfFt) may be similarly defined for $\hat{\psi}(\omega)$ by limiting the frequency integral with a window,

$$g(w)=\Theta(\omega-\Delta\omega)\Theta(-\omega-\Delta\omega). \tag{69}$$

The corresponding spectrogram S' is obtained as the square modulus of the sfFt. The two spectrograms, S and S', are, however, not equal because the window functions h and g are not Fourier transforms of each other. In particular, note that the spectrogram S' may be equivalently obtained from a sfFt analysis for an initially sharp onset signal, or as the density that results from a source with a smooth onset. [The density of $\psi(x,t)$ in Eq. (35) is proportional, up to a trivial normalization constant, to $S'(t,\omega_0;x)$.] As a consequence, $S'(t,\omega_0)$ peaks at $t=0$ after an infinite time growth whereas $S(t,\omega_0)$ is strictly zero at $t<-T/2$ and its main transient part peaks around τ. The qualitative behavior is different because of the different window functions, even though the inequalities used here or in Sec. III, Eqs. (55) and (34), are in fact identical if one identifies $T=2\pi/\Delta\omega$; compare Fig. 8 and the upper curve of Fig. 4 where the values of τ, T, and T_0 are equal. These inequalities imply in both cases that the pole contribution can be entirely neglected at or around τ, and that it will only be of importance at a time that depends exponentially on $\kappa_0 x$.

We have tested the time-frequency Wigner function, too. This representation separates much more clearly the saddle and pole contributions, but it also associates with the latter an initial time $t=0$ rather than $t=\tau$, and presents the inconvenience of a very rapidly oscillating pattern and strong interference terms.

V. SUMMARY AND DISCUSSION

The time dependence of evanescent Schrödinger waves created by a point source has been investigated, combining analytical or numerical exact results and approximate expressions. The background of the former allows us to test and contrast the validity of the simplified description of the latter. We have also performed a time-frequency analysis of the transients which precede the stationary regime by means of spectrograms.

An important aspect of the work is the elucidation of the role played by the different parameters, in particular by the ''traversal'' time τ. It is a basic parameter that determines the global shape of the wave but at this time, in semiclassical conditions $\kappa_0 x>1$, the monochromatic front (with the main frequency of the source) is not observed in the total wave because of the dominance of the saddle-point contribution. However, for the source with a sharp onset we have identified a transient front whose maximum peak arises at a time $\tau/3^{1/2}$. The dominant frequency of this front does not correspond to the main frequency of the source ω_0, but to the mean saddle-point frequency (above or at the cutoff frequency). The time $t_{tr}>\tau$ that determines the duration of the transient, or the passage to the asymptotic regime, has also been identified. Frequency-band-limited sources accelerate the crossover to the stationary regime but there is still a transient dominated by the upper frequency contained in the band. The spectrogram $S(t,\omega;x)$ has been also investigated to show the variation with time of the frequency components. In this representation the main contribution at the frequency ω_0 arrives at x around the traversal time τ. This main contribution is a transient due to the saddle point. At an exponentially long time the pole term will eventually take over and remain as the dominant contribution in the stationary regime.

In fact it is possible to see the monochromatic wave front arriving around the traversal time τ, but only when the semiclassical conditions are abandoned, and with an accuracy which is never better than the traversal time itself. This occurs if the point source starts the emission abruptly, but also

when it is switched on gradually (limiting the frequency band), or for a limited-frequency-band detector, whose response is modeled here with a spectrogram. The coincidence of all these cases strongly suggests that the limitation of the accuracy to measure τ is in fact a general property.

ACKNOWLEDGMENTS

We are indebted to Harry Thomas who through discussions during the work of Ref. [14] has also strongly influenced the direction of this work. Discussions with L. Cohen and I. L. Egusquiza are also acknowledged. J. G. M. was supported by MEC Grant No. (PB97-1492), and in Geneva, where most of this work was carried out, by the Swiss National Science Foundation. M.B. is supported by the Swiss National Science Foundation.

APPENDIX A: INTEGRALS

In this appendix we shall solve the integrals of the form

$$\mathcal{I}=\int_{\Gamma_+} dk \frac{e^{-i(ak^2+kb)}}{k-k_0}, \quad a>0 \tag{A1}$$

where Γ_+ goes from $-\infty$ to ∞ passing *above* the pole at $k=k_0$. The saddle point of the exponent is at $k=-b/2a$ and the steepest descent path is the straight line $k_I=-(k_R+b/2a)$. The original contour is at the border between the hill and valley and can be deformed into this path, taking into account the residue of the pole when $\mathrm{Im}(k_0)<-[\mathrm{Re}(k_0)+b/2a]$. By completing the square and introducing the new variable

$$u=u(k)=\frac{1+i}{2^{1/2}}a^{1/2}(k+b/2a), \tag{A2}$$

the integral takes the form

$$\mathcal{I}=e^{i(b^2/4a)}\left\{\int_{-\infty}^{\infty}\frac{e^{-u^2}}{u-u_0}du-2i\pi e^{-u_0^2}\Theta[\mathrm{Im}(u_0)]\right\}, \tag{A3}$$

where $u_0=u(k=k_0)$. Note that the variable u has its origin at the saddle point and its real axis corresponds to the steepest descent line. Using Eqs. (B2) and (B3) it can be finally written as

$$\mathcal{I}=-i\pi e^{i(b^2/4a)}w(-u_0). \tag{A4}$$

APPENDIX B: PROPERTIES OF $w(z)$

The w function [15,16] is an entire function defined in terms of the complementary error function as

$$w(z)=e^{-z^2}\,\mathrm{erfc}(-iz). \tag{B1}$$

$w(z)$ is frequently recognized by its integral expression

$$w(z)=\frac{1}{i\pi}\int_{\Gamma_-}\frac{e^{-u^2}}{u-z}du, \tag{B2}$$

where Γ_- goes from $-\infty$ to ∞ passing below the pole at z. For $\mathrm{Im}\,z>0$ this corresponds to an integral along the real axis. For $\mathrm{Im}\,z<0$ the contribution of the residue has to be added, and for $\mathrm{Im}\,z=0$ the integral becomes the principal part contribution along the real axis plus half the residue. From Eq. (B2) two important properties are deduced,

$$w(-z)=2e^{-z^2}-w(z) \tag{B3}$$

and

$$w(z^*)=[w(-z)]^*. \tag{B4}$$

To obtain an asymptotic series as $z\to\infty$ for $\mathrm{Im}\,z>0$ one may expand $(u-z)^{-1}$ around the origin (the radius of convergence is the distance from the origin to the pole, $|z|$) and integrate term by term. This provides

$$w(z)\sim\frac{i}{\sqrt{\pi}z}\left[1+\sum_{m=1}^{\infty}\frac{1\times3\cdots\times(2m-1)}{(2z^2)^m}\right], \quad \mathrm{Im}\,z>0 \tag{B5}$$

which is a uniform expansion in the sector $\mathrm{Im}\ z>0$. For the sector $\mathrm{Im}\,z<0$ Eq. (B3) gives

$$w(z)\sim\frac{i}{\sqrt{\pi}z}\left[1+\sum_{m=1}^{\infty}\frac{1\times3\times\cdots\times(2m-1)}{(2z^2)^m}\right]+2e^{-z^2}, \quad \mathrm{Im}\,z<0. \tag{B6}$$

If z is in one of the bisectors then $-z^2$ is purely imaginary and the exponential becomes dominant. But right at the crossing of the real axis, $\mathrm{Im}\ z=0$, the exponential term is of order $o(z^{-n})$ (all n), so that Eqs. (B5) and (B6) are asymptotically equivalent as $|z|\to\infty$. One may insist, however, in removing the discontinuity of the series expansion (as a function of z) around the real axis. This can be done by adding a correction to the saddle contribution that takes into account the region close to the pole in the line integral, see also the discussion in Ref. [14]. Note that in Eq. (B5) only the region around the origin contributes. Consider now also the region around the pole,

$$\int_{z_R-\Delta}^{z_R+\Delta}\frac{e^{-u^2}}{u-z}du\approx e^{-z^2}\int_{z_R-\Delta}^{z_R+\Delta}\frac{du}{u-z}=e^{-z^2}\ln\left(\frac{z_R+\Delta-z}{z_R-\Delta-z}\right). \tag{B7}$$

For large $|z|$ and in the proximity of the real axis this may be approximated by $e^{-z^2}i\pi\,\mathrm{sgn}\,(z)$ which exactly cancels the discontinuity between Eqs. (B5) and (B6).

APPENDIX C: TIME DEPENDENCE OF THE FREQUENCY-BAND-LIMITED SOURCE

The time dependence of the frequency-band-limited amplitude at $x=0$ is obtained from (32) by Fourier transform

$$\psi(x=0,t)=\frac{1}{2\pi}\int_{\omega_0-\Delta\omega}^{\omega_0+\Delta\omega}d\omega\frac{ie^{-i\omega t}}{\omega-\omega_0+i0}$$

$$=\frac{1}{2}e^{-i\omega_0 t}+\frac{1}{2\pi}\mathrm{P}\int_{\omega_0-\Delta\omega}^{\omega_0+\Delta\omega}\frac{ie^{-i\omega t}}{\omega-\omega_0}. \quad \text{(C1)}$$

Using the frequency $\omega'=(\omega-\omega_0)t$,

$$\mathrm{P}\int_{\omega_0-\Delta\omega}^{\omega_0+\Delta\omega}d\omega\frac{e^{-i\omega t}}{\omega-\omega_0}=e^{-i\omega_0 t}\mathrm{P}\int_{-t\Delta\omega}^{t\Delta\omega}d\omega'\frac{e^{-i\omega'}}{\omega'}, \quad \text{(C2)}$$

and the principal part integral can be expressed by contour deformation in terms of combinations of exponential integrals [20],

$$\mathrm{P}\int_{-b}^{a}dY\frac{e^{-iY}}{Y}=E_1(-ib)-E_1(ia)-i\pi, \quad a,b>0 \quad \text{(C3)}$$

where

$$E_1(z)=\int_z^\infty dY\frac{e^{-Y}}{Y}, \quad |\arg z|<\pi \quad \text{(C4)}$$

(the contour does not cross the negative real axis). Finally, using Eq. (C3), (C1) can be written for all t

$$\psi(x=0,t)=e^{-i\omega_0 t}\left\{\Theta(t)-\frac{1}{\pi}\mathrm{Im}[E_1(-i\Delta\omega t)]\right\}. \quad \text{(C5)}$$

APPENDIX D: RELATIVISTIC CASE

Defining the dimensionless parameter c by combining the dimensional velocity of light C, the mass, and the potential constant as

$$c=C(2m/V)^{1/2}, \quad \text{(D1)}$$

the dispersion relation for a Klein-Gordon wave equation takes the form

$$\Omega^2=(\omega-1)^2=(c^2/2)^2+c^2k^2. \quad \text{(D2)}$$

For evanescent conditions k is purely imaginary, $k=i\kappa$. In particular, for $\omega=\omega_0$ or $(\Omega=\Omega_0)$, κ_0 cannot take arbitrarily large values, $0<\kappa_0<c/2$, contrast this with the nonrelativistic case where there is no upper limit.

For a source with a sharp onset the wave function is [14]

$$\psi(x,t)=\frac{i}{2\pi}e^{-it}\int_{-\infty}^{\infty}\frac{1}{\Omega-\Omega_0+i0}e^{-i(\Omega t-kx)}d\Omega, \quad \text{(D3)}$$

which is zero for $t<x/c$. There are now two saddle points at

$$\pm\Omega_s=\pm\frac{c^2t}{2\theta}, \quad \text{(D4)}$$

$$\theta\equiv(t^2-x^2/c^2)^{1/2}, \quad \text{(D5)}$$

and two branch cuts. The integration contour may be deformed along the two steepest descent paths. The pole is crossed at [14]

$$\tau=\frac{x}{2\kappa_0}. \quad \text{(D6)}$$

Note the lower bound $x/c<\tau$ when $\Omega\to 0$ (or $\kappa_0\to c/2$). Consequently the traversal time is strictly limited by the velocity of light [14].

We shall only discuss the contribution from the saddle at $+\Omega_s$ corresponding to the excitation of particles [14] ,

$$\psi_s^+(x,t)=\frac{ix}{c^2t}\left(\frac{-i}{\pi\theta}\right)^{1/2}\frac{\Omega_s}{\Omega_s+\Omega_0}e^{-i[t+(c/2)(c^2t^2-x^2)^{1/2}]}$$

$$\times\Theta(ct-x). \quad \text{(D7)}$$

Linearizing the square root of the exponent to evaluate the short-time Fourier transform of the saddle-wave function (D7), one obtains

$$S_s(t,\omega;x)=\frac{2x^2}{\pi^2Tc^4t^2\theta}\frac{\Omega_s^2}{(\Omega_s+\Omega_0)^2}\frac{\sin^2[(\Omega-\Omega_0)T/2]}{(\Omega-\Omega_s)^2}$$

$$(t>T/2+x/c). \quad \text{(D8)}$$

In this case the maximum of the envelope as a function of t is given by

$$t_{en}=\frac{\tau}{3^{1/2}}\left[1+3\left(\frac{\Omega_0^2}{c^2/2}\right)^2\right]^{1/2}. \quad \text{(D9)}$$

Because of the dispersion relation $\Omega_0\leqslant c^2/2$ in the evanescent case, it follows that t_{en} is bounded by $\tau/3^{1/2}$ and $(4/3^{1/2})\tau$.

[1] L. Brillouin, in *Wave Propagation and Group Velocity* (Academic Press, New York, 1960).

[2] Proceedings of the Workshop on Superluminal(?) Velocities, edited by P. Mittelstaedt and G. Nimtz [Ann. Phys. (Leipzig) **7**, 591 (1998)].

[3] The numerical value of ω should not be overinterpreted. Only energy differences and the differences between the corresponding frequencies are invariant with respect to shifts of the origin and are physically significant.

[4] K. W. H. Stevens, Eur. J. Phys. **1**, 98 (1980); J. Phys. C **16**, 3649 (1983).

[5] P. Moretti, Phys. Scr. **45**, 18 (1992).

[6] M. Büttiker and R. Landauer, Phys. Rev. Lett. **49**, 1739 (1982).

[7] M. Büttiker, Phys. Rev. B **27**, 6178 (1983).

[8] S. Brouard and J. G. Muga, Phys. Rev. A **54**, 3055 (1996).

[9] A. Ranfagni, D. Mugnai, P. Fabeni, and P. Pazzi, Phys. Scr. **42**, 508 (1990).
[10] A. Ranfagni, D. Mugnai, and A. Agresti, Phys. Lett. A **158**, 161 (1991).
[11] N. Teranishi, A. M. Kriman, and D. K. Ferry, Superlattices Microstruct. **3**, 509 (1987).
[12] A. P. Jauho and M. Jonson, Superlattices Microstruct. **6**, 303 (1989).
[13] K. E. Oughstun and G. C. Sherman, *Electromagnetic Pulse Propagation in Causal Dielectrics* (Springer, Berlin, 1997).
[14] M. Büttiker and H. Thomas, Ann. Phys. (Leipzig) **7**, 602 (1998); Superlattices Microstruct. **23**, 781 (1998).
[15] *Handbook of Mathematical Functions*, edited by M. Abramowitz and I. A. Stegun (Dover, New York, 1972).
[16] V. N. Faddeyeva and N. M. Terentev, *Tables of the Probability Integral for Complex Argument* (Pergamon Press, New York, 1961).
[17] Writing $\psi=|\psi|e^{i\phi}$ the local average instantaneous frequency is defined as [19]

$$\overline{\omega}(x)\equiv-\frac{\partial\phi(x,t)}{\partial t}.$$

Note that in this work the convention of signs for Fourier transforms and for $\overline{\omega}(x)$ is different from the one in [19].
[18] N. Bleistein and R. Handelsman, *Asymptotic Expansions of Integrals* (Dover, New York, 1986).
[19] L. Cohen, *Time-Frequency Analysis* (Prentice-Hall, Englewood Cliffs, NJ, 1995); Ann. (N.Y.) Acad. Sci. **808**, 97 (1997); Proc. SPIE **3069**, 2 (1997).
[20] J. G. Muga, V. Delgado, R. Sala, and R. F. Snider, J. Chem. Phys. **104**, 7015 (1996).